# Chapter 4: A Look at Membrane and Thin Plate Theory

## 4.1 Introduction

The key to designing an effective controller for an ultra-large, ultra-flexible optic is the accurate modeling of the system dynamics present. An accurate model helps the control engineer to understand the fundamental states of the system, such as locations of maximum strain, acceleration, or velocity, to name but a few. By understanding the locations and magnitudes of the system states through a well-developed model, a controller well-suited to the undesirable dynamical states of the system can be designed, tested, and implemented to create a desirable system.

Of primary concern with regards to the space optic is the nature of its dynamics—is it a thin plate or a membrane? Our choice in this regard will have a significant impact on the type of sensors and actuators suitable for optical level control of the imaging surface. Further, our choice will also have significant consequences on the type and extent of dynamics possible from our model of the imaging surface. The following sections will outline a brief history on the development of thin plate and membrane theory, and then conclusions will be drawn to discern the best modeling medium for the dynamics governing a large, flexible space optic.

## 4.2 History of the Development of Plate Theory

Tracing the family tree of plate theory to its roots, one travels back to the American Revolution time period and finds Euler performing free vibration analyses of plate problems (Euler, 1766). Chladni, a German physicist, performed experiments on horizontal plates to quantify their vibratory modes. He sprinkled sand on the plates, struck them with a hammer, and noted the regular patterns that formed along the nodal lines (Chladni, 1802). Bernoulli then attempted to theoretically justify the experimental results of Chladni using the previously developed Euler-Bernoulli bending beam theory, but his results did not capture the full dynamics (Bernoulli, 1789). The French

mathematician Germain developed a plate differential equation that lacked a warping term (Germain, 1826), but one of the reviewers of her work, Lagrange (1828), corrected Germain's results; "thus, he was the first person to present the general plate equation properly" (Ventsel and Krauthammer, 2001).

Cauchy (1828) and Poisson (1829) developed the problem of plate bending using general theory of elasticity. Then, in 1829, Poisson successfully expanded "the Germain-Lagrange plate equation to the solution of a plate under static loading. In this solution, however, the plate flexural rigidity $D$ was set equal to a constant term" (Ventsel and Krauthammer, 2001). Navier (1823) considered the plate thickness in the general plate equation as a function of rigidity, $D$.

Some of the greatest contributions toward thin plate theory came from Kirchhoff's thesis in 1850 (Kirchhoff, 1850). Kirchhoff declared some basic assumptions that are now referred to as "Kirchhoff's hypotheses." Using these assumptions, Kirchhoff: simplified the energy functional for 3D plates; demonstrated, under certain conditions, the Germain-Lagrange equation as the Euler equation; and declared that plate edges can only support two boundary conditions (Ventsel and Krauthammer, 2001). Lord Kelvin (Thompson) and Tait (1883) showed that plate edges are subject to only shear and moment forces.

Kirchhoff's hypotheses are fundamental assumptions in the development of linear, elastic, small-deflection theory for the bending of thin plates. These assumptions are re-stated here from Ventsel and Krauthammer (2001):

1. The material of the plate is elastic, homogenous, and isotropic.
2. The plate is initially flat.
3. The deflection (the normal component of the displacement vector) of the midplane is small compared with the thickness of the plate. The slope of the deflected surface is therefore very small and the square of the slope is a negligible quantity in comparison with unity.

4. The straight lines, initially normal to the middle plane before bending, remain straight and normal to the middle surface during the deformation, and the length of such elements is not altered. This means that the vertical shear strains $\gamma_{xy}$ and $\gamma_{yz}$ are negligible and the normal strain $\varepsilon_z$ may also be omitted. This assumption is referred to as the "*hypothesis of straight normals*."
5. The stress normal to the middle plane, $\sigma_z$, is small compared with the other stress components and may be neglected in the stress-strain relations.
6. Since the displacements of the plate are small, it is assumed that the middle surface remains unstrained after bending.

These points, 1 – 6, are the foundation for plate bending theory that is usually referred to as the *classical* or *Kirchhoff's plate theory*. Figure 4.1 shows a representative plate geometry.

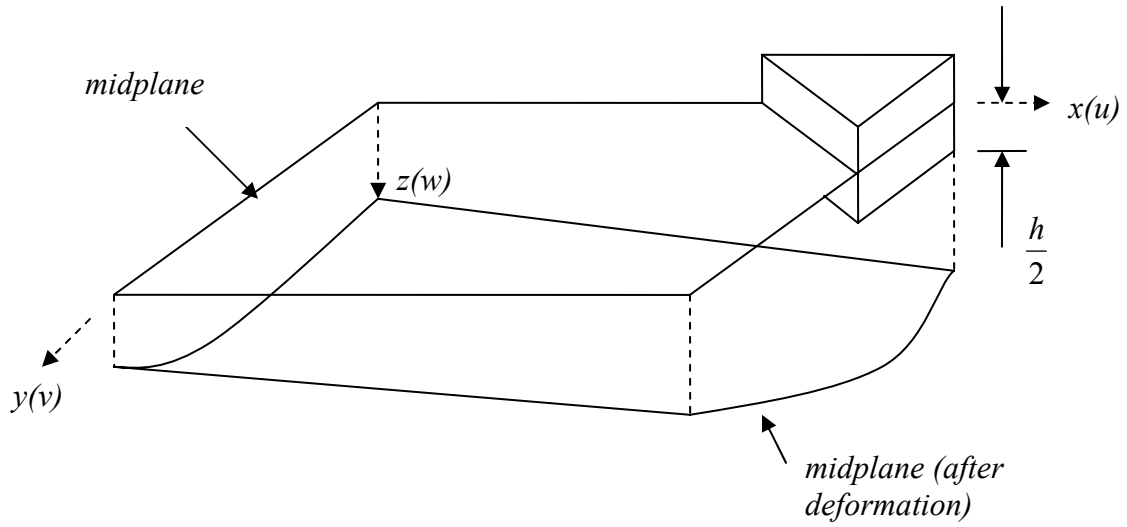


**Figure 4.1**. Sample plate geometry showing the midplane, or middle surface, and typical Cartesian coordinate axes.

Thin plates are usually characterized by the ratio $a / h$ (the ratio between the length of a side, $a$, and the thickness of the material, $h$, falling between the values of 8 and 80

(Ventsel and Krauthammer, 2001). Under Kirchhoff's hypotheses, the governing equation of motion can be derived for small deflections in thin plates as:

$$D\left[\frac{\partial^4 w(x,y,t)}{\partial x^4} + 2\frac{\partial^4 w(x,y,t)}{\partial x^2 \partial y^2} + \frac{\partial^4 w(x,y,t)}{\partial y^4}\right] = \rho h \frac{\partial^2 w(x,y,t)}{\partial t^2} \tag{4.1}$$

where $w(x,y,t)$ is the deflection of the plate, $\rho$ is the density, $h$ is the plate's thickness, and $D$ is the flexural rigidity of the plate. Sometimes, Equation 4.1 is written as

$$\nabla^4 w(x,y,t) = \rho h w_{tt}(x,y,t) \tag{4.2}$$

where, in Cartesian coordinates,

$$\nabla^4(\cdot) \equiv \frac{\partial^4}{\partial x^4} + 2\frac{\partial^4}{\partial x^2 \partial y^2} + \frac{\partial^4}{\partial y^4}\,. \tag{4.3}$$

$\nabla^4(\cdot)$ is called the *biharmonic operator*.

Levy (1899) successfully solved the rectangular plate problem of two parallel edges simply-supported with the other two edges of arbitrary boundary condition. Meanwhile, in Russia, Bubnov (1914) investigated the theory of flexible plates, and was the first to introduce a plate classification system. Bubnov composed tables "of maximum deflections and maximum bending moments for plates of various properties" (Ventsel and Krauthammer, 2001). Galerkin (1933) then further developed Bubnov's theory and applied it to various bending problems for plates of arbitrary geometries.

Timoshenko (1913, 1915) provided a further boost to the theory of plate bending analysis; most notably, his solutions to problems considering large deflections in circular plates and his development of elastic stability problems. Timoshenko and Woinowsky-Krieger (1959) wrote a textbook that is fundamental to most plate bending analysis

performed today. Hencky (1921) worked rigorously on the theory of large deformations and the general theory of elastic stability of thin plates. Föppl (1951) simplified the general equations for the large deflections of very thin plates. The final form of the large deflection thin plate theory was stated by von Karman, who had performed extensive research in this area previously (1910). The von Karman equations (1910) governing the large deflections of thin plates are given by:

$$\begin{aligned}
&\frac{\partial^4 \Phi}{\partial x^4} + 2\frac{\partial^4 \Phi}{\partial x^2 \partial y^2} + \frac{\partial^4 \Phi}{\partial y^4} = Eh\left[\left(\frac{\partial^2 w}{\partial x \partial y}\right)^2 - \frac{\partial^2 w}{\partial x^2}\frac{\partial^2 w}{\partial y^2}\right] \\
&\frac{\partial^4 w}{\partial x^4} + 2\frac{\partial^4 w}{\partial x^2 \partial y^2} + \frac{\partial^4 w}{\partial y^4} = \frac{1}{D}\left(p + \frac{\partial^2 \Phi}{\partial y^2}\frac{\partial^2 w}{\partial x^2} + \frac{\partial^2 \Phi}{\partial x^2}\frac{\partial^2 w}{\partial y^2} - 2\frac{\partial^2 \Phi}{\partial x \partial y}\frac{\partial^2 w}{\partial x \partial y}\right)
\end{aligned} \tag{4.4}$$

where *w(x,y)* is the deflection of the plate, $\Phi$ is the stress function, *E* is the Young's modulus, *h* is the plate's thickness, *p* is an applied pressure, and *D* is the flexural rigidity. These equations are coupled, non-linear, partial differential equations, both of which are fourth order. Unfortunately, this also makes them extremely difficult to solve analytically. For the present time, we will limit our discussion to Kirchhoff's plate theory.

### 4.3 Development of Membrane Theory

Membranes could be considered a simplified plate, and hence, formal theory of membrane mechanics developed concurrently with the theory of thin plates. A primary indication of membrane dynamics is given by the ratio $a / h$ falling between 80 and 100. In 1907, Föppl derived equilibrium equations for a membrane plate. Essentially, Föppl's derived equations were modified von Karman plate equations (Equations 4.4) with the bending rigidity set to zero (Marker and Jenkins, 1997). Hencky (1915) investigated the problem of an initially planar membrane with circular boundary conditions inflated by a uniform pressure. He also assumed that the flexural stiffness, *D*, in the thin plate equations was zero. As noted by Marker and Jenkins (1997), research into the Hencky problem didn't reemerge until the 1940's, when Stevens (1944) experimentally investigated the inflation of a cellulose acetate butyrate circular membrane. Cambell

(1967) researched the response of an inflated membrane with a given initial tension, and his results were in agreement with experimental data provided by Weil and Newark (1955).

To be considered a true membrane, a structure must satisfy the following conditions, summarized from Ventsel and Krauthammer (2001):

1. The boundaries are free from transverse shear forces and moments. Loads applied to the boundaries must lie in planes tangent to the middle surface.
2. The normal displacements and rotations at the edges are unconstrained: that is, these edges can displace freely in the direction of the normal to the middle surface.
3. A membrane must have a smoothly varying, continuous surface.
4. The components of the surface and edge loads must also be smooth and continuous functions of the coordinates.

From these four basic assumptions, we arrive at two (related) characterizations of membranes, namely:

1. Membranes do not have any flexural rigidity, and therefore cannot resist any bending loads.
2. Membranes can only sustain tensile loads. Their inability to sustain compressive loads leads to the phenomenon known as wrinkling.

Further insight into the difference between plates and membranes can be garnered by looking at the equation that describes the flexural rigidity of a plate, namely:

$$D = \frac{Eh^3}{12(1-\upsilon^2)}, \tag{4.5}$$

where $E$ is the elastic modulus of the material, $h$ is the thickness of the material, and $\upsilon$ is Poisson's ratio. Figure 4.2 depicts a cross-section of a structural element.

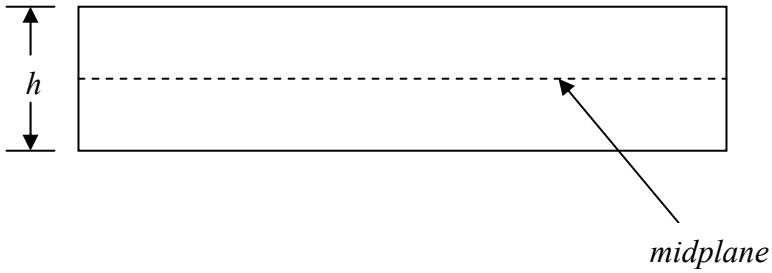


**Figure 4.2**. Cross-sectional view of a structural element.

Notice that as the thickness, $h$, of the element in Figure 4.2 approaches the negligible thickness of the midplane, the flexural rigidity $D$, as given in Equation 4.5 approaches zero. Such a limit visually depicts the transitioning of a structural element from a thin plate to a membrane. Conversely, as $h$ increases such that the ratio between a side of length $a$ to the thickness $h$ is less than 10, such a structural element is referred to as a thick plate (Vantsel and Krauthammer, 2001). A graphic of these distinguishing limits is provided in Figure 4.3.

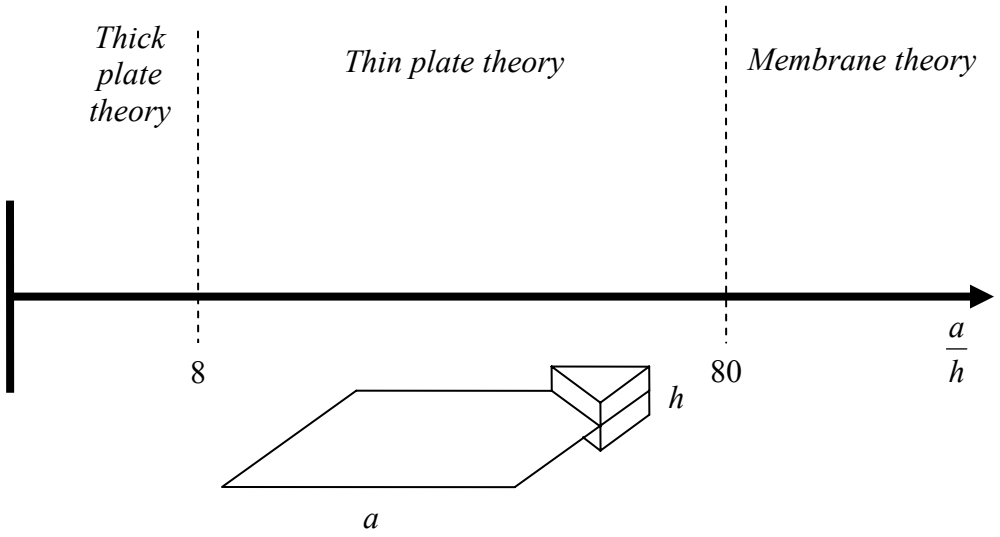


**Figure 4.3.** The distinguishing limits separating thick plate, thin plate, and membrane theory. The characterization of each stems from the ratio between a given side of length *a* and the element's thickness, *h*.

The next section will derive the dynamic equations of motion for circular and rectangular membranes undergoing free vibration. In particular, the equations will be developed in both polar as well as Cartesian coordinates as these forms will prove fruitful in subsequent analyses.

### 4.3.1 Equation of Motion for a Circular Membrane in Polar Coordinates

To begin our derivation of the equation of motion for a circular membrane in polar coordinates, we first start with a drawing of the system under consideration. A drawing of a circular membrane subject to uniform tension is given in Figure 4.4.

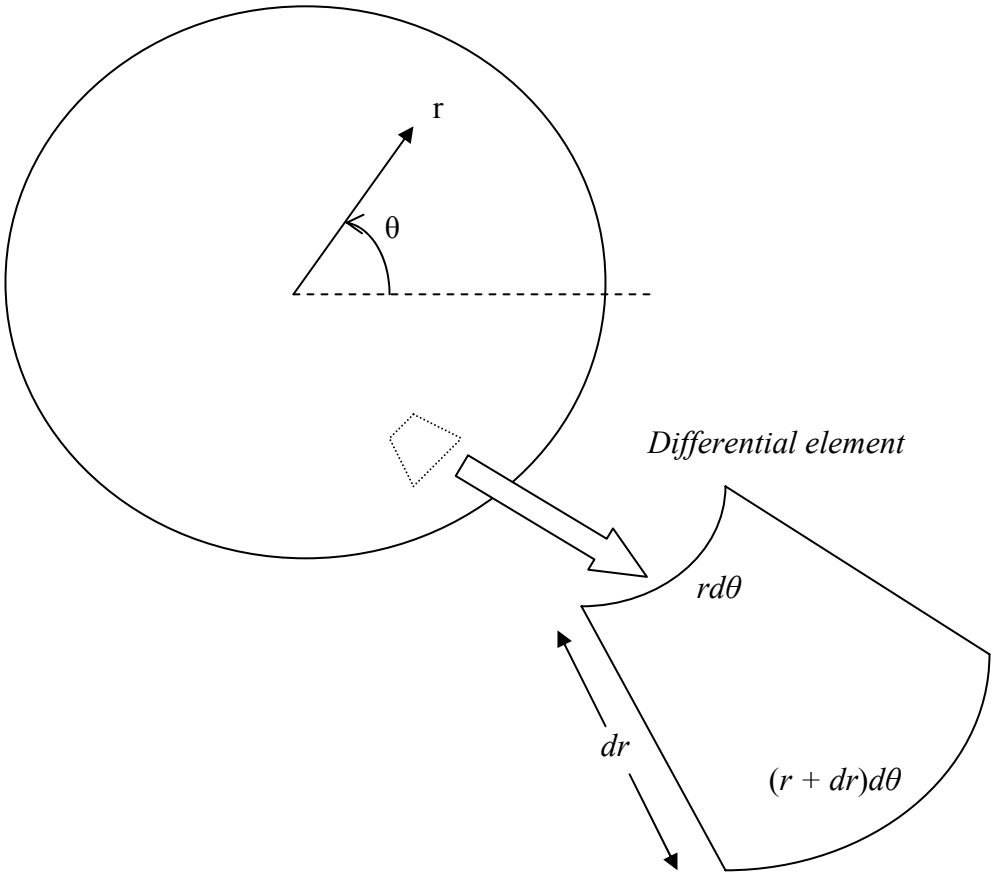


**Figure 4.4**. A drawing of a planar membrane surface (top) and a differential element for analysis purposes (lower right).

We will consider deflections of the membrane depicted in Figure 4.4 to be normal to the plane (that is, either into or out of the plane of the page). The deflections of the planar membrane from its equilibrium position will be considered the $\eta$-direction. Since we are dealing with a membrane, a force acting normal to the surface of the membrane (in the $\eta$-direction) will cause the membrane to bulge in that direction and reach a new equilibrium state. The restoring force present in the membrane is the in-plane tension only. Note that if we were modeling this structure as a thin plate, then there would be a small but finite flexural rigidity present, and thus stresses would develop along the thickness of the element. Such is not the case for a membrane.

Assuming a uniform thickness and a uniform tension, $P$ (in units of force per unit length), applied by the circular boundary given in Figure 4.4, a free body diagram of the differential element is shown in Figure 4.5.

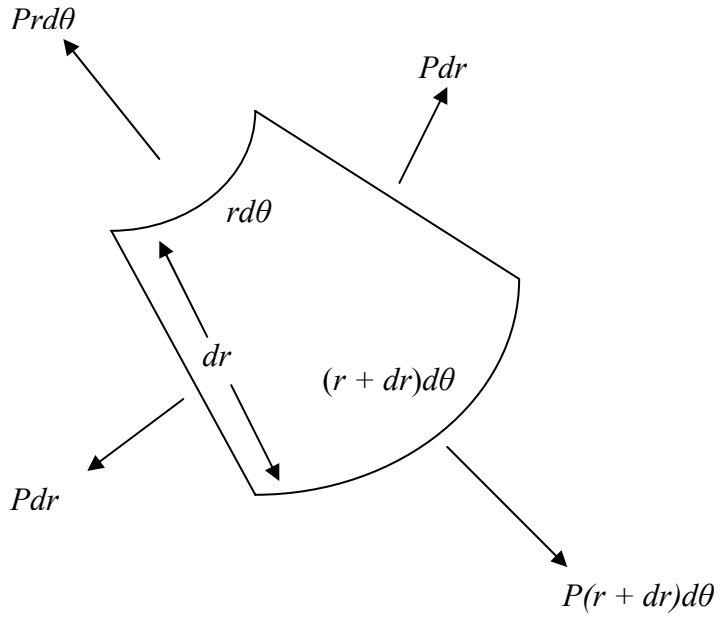


**Figure 4.5**. Free body diagram of the forces acting perpendicular and parallel to the radius in a differential element.

Next, we will use Newton's second law to perform a force balance on the differential element given in Figure 4.5. First, we examine the forces in the $r - \eta$ *plane*, as shown in Figure 4.6.

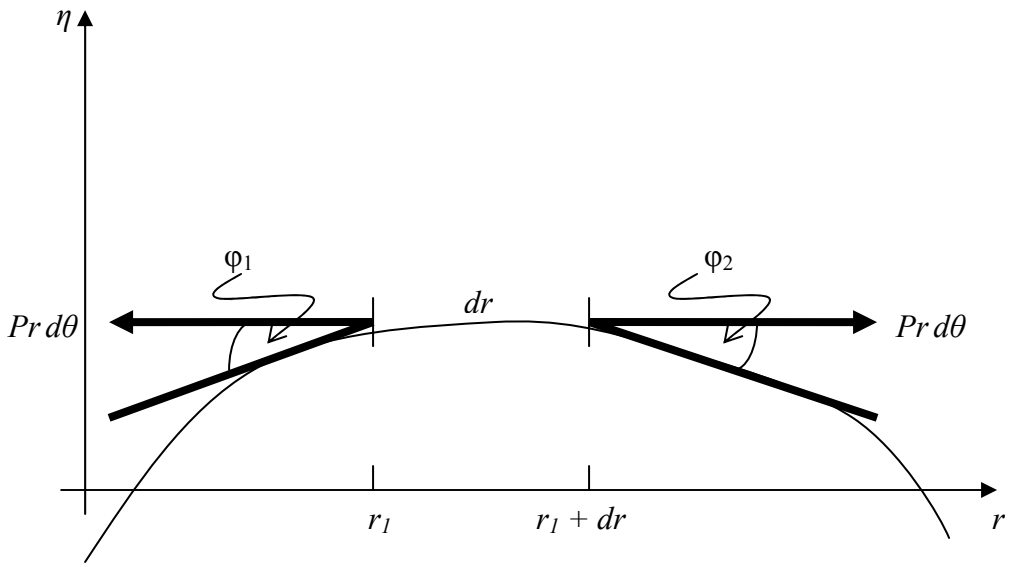


**Figure 4.6.** The displaced membrane in the $r - \eta$ *plane*.

From Figure 4.6, the next step is to find the forces acting on the displaced membrane in the $\eta$-direction. Summing the forces acting in the $\eta$-direction yields:

$$\sum F_r = -Pd\theta\, r \sin\varphi_1 + Pd\theta\, r \sin\varphi_2 \tag{4.6}$$

Next, we assume small angle deflections, and consequently,

$$r \sin\varphi_1 \approx r \tan\varphi_1 = r \frac{\partial \eta(r,\theta,t)}{\partial r}\Big|_{r_1} \tag{4.7}$$

and

$$r \sin\varphi_2 \approx r \tan\varphi_1 = r \frac{\partial \eta(r,\theta,t)}{\partial r}\Big|_{r=r_1+dr} \tag{4.8}$$

If we expand Equation 4.8 around the point $r_1$ using a Taylor series from calculus, then we can approximate the slope as

$$\left( r\frac{\partial \eta}{\partial r} \right)|_{r_1+dr} = \left( r\frac{\partial \eta}{\partial r} \right)|_{r_1} + dr\frac{\partial}{\partial r}\left( r\frac{\partial \eta}{\partial r} \right)|_{r_1} + h.o.t. \tag{4.9}$$

Plugging these approximations (and neglecting the higher order terms) into Equation 4.9 yields

$$\sum F_r = -Pd\theta\left( r\frac{\partial \eta}{\partial r} \right)|_{r_1} + Pd\theta\left( r\frac{\partial \eta}{\partial r} \right)|_{r_1} + Pd\theta\, dr\frac{\partial}{\partial r}\left( r\frac{\partial \eta}{\partial r} \right)|_{r_1} \tag{4.10}$$

Some terms cancel each other out in Equation 4.10, leaving behind:

$$\sum F_r = P\frac{\partial}{\partial r}\left( r\frac{\partial \eta}{\partial r} \right)d\theta\, dr \tag{4.11}$$

Next, we can perform the same analysis for those forces displacing the membrane in the $\theta$-$\eta$ plane. First, we draw a representative diagram in the $\theta$-$\eta$ plane (Figure 4.7).

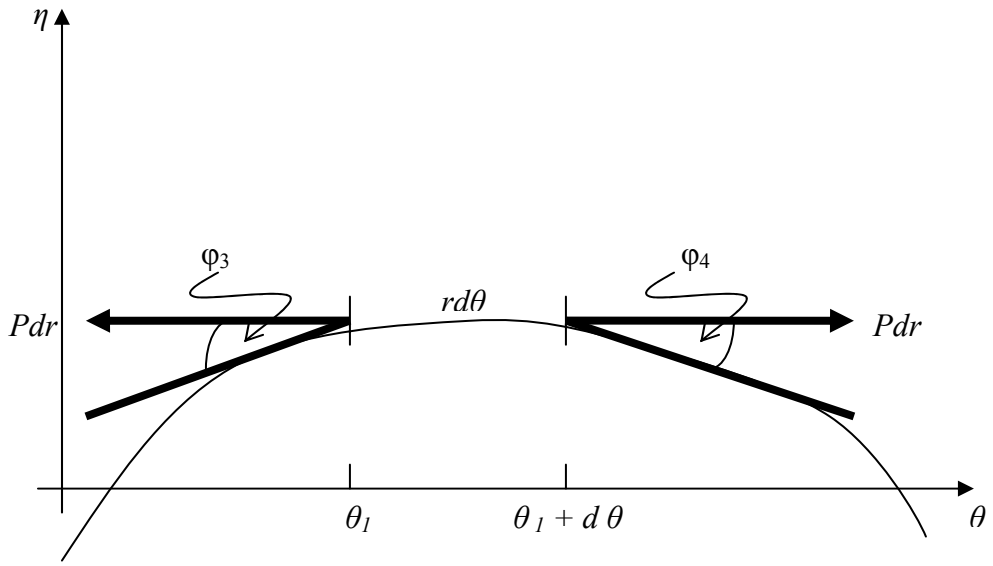


**Figure 4.7**. The displaced membrane in the $\theta$-$\eta$ plane.

Following the same procedure as just outlined, we find the restoring forces to be

$$\sum F_\theta = -P\,dr\sin\varphi_3 + P\,dr\sin\varphi_4 \tag{4.12}$$

Assuming small angular deflections and using the Taylor series approximation to the slope around the point $\theta_1$ yields

$$\sum F_\theta = -P\,dr\frac{\partial\eta}{r\partial\theta} + P\,dr\frac{\partial\eta}{r\partial\theta} + Pdr\frac{\partial^2\eta}{r\partial\theta^2}d\theta \tag{4.13}$$

Or, upon further simplification,

$$\sum F_\theta = \frac{P}{r}\frac{\partial^2\eta}{\partial\theta^2}d\theta dr \quad . \tag{4.14}$$

Now that the restoring forces acting on the displaced membrane have been calculated, the dynamic equation governing the vibrating membrane can be found using Newton's second law. If $\sigma$ is the mass per unit area of the membrane material, then the mass of the differential element is given by

$$mass = \sigma\int_\theta\int_r rdrd\theta = \sigma\, rdrd\theta\,. \tag{4.15}$$

Finally, summing together the restoring forces and performing a force balance yields

$$\frac{P}{r}\frac{\partial}{\partial r}\left(r\frac{\partial\eta}{\partial r}\right)rdrd\theta + \frac{P}{r^2}\frac{\partial^2\eta}{\partial\theta^2}rdrd\theta = \sigma\, rdrd\theta\frac{\partial^2\eta}{\partial t^2} \quad . \tag{4.16}$$

Performing a further simplification on Equation 4.16 gives us

$$\frac{1}{r}\frac{\partial}{\partial r}\left(r\frac{\partial\eta}{\partial r}\right) + \frac{1}{r^2}\frac{\partial^2\eta}{\partial\theta^2} = \frac{\sigma}{P}\frac{\partial^2\eta}{\partial t^2}\,. \tag{4.17}$$

Equation 4.17 is the equation of motion for the transverse vibration of a planar membrane in polar coordinates. To put Equation 4.17 in similar form as Equation 4.2, we get

$$\nabla^2 \eta = \frac{1}{c^2} \frac{\partial^2 \eta}{\partial t^2}, \tag{4.18}$$

where $c = \sqrt{\frac{P}{\sigma}}$ . Notice the similarities between the developments of the membrane equation in comparison to the derivation of the string equation (see, for example, Inman (2001)). This should not come as any surprise, as a membrane may be considered a two dimensional string.

### 4.3.2 Equation of Motion for a Rectangular Membrane in Cartesian Coordinates

The derivation of the equation of motion for a rectangular membrane in Cartesian coordinates is similar to the derivation as presented in the previous section for polar coordinates. A sample geometry (under constant tension) and differential element are shown in Figure 4.8.

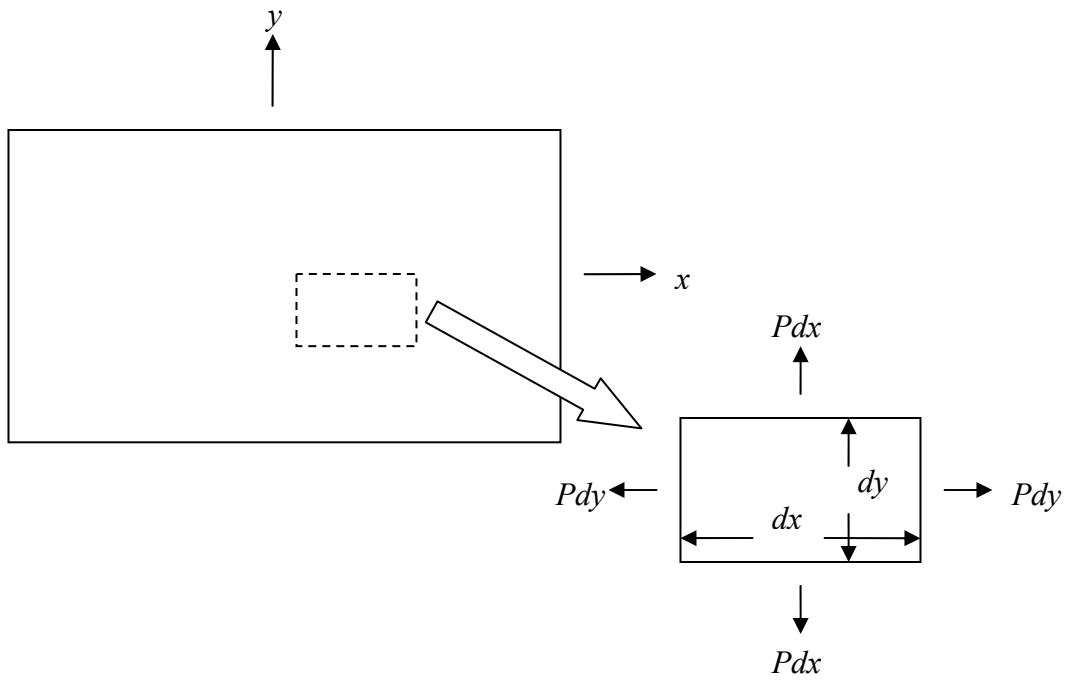


**Figure 4.8**. A drawing of a planar membrane surface (top) and a differential element with free body diagram for analysis purposes (lower right).

Following the same procedure as outlined previously, we sum up the forces in the $x$ and $y$ directions and set these equal to the mass of the differential element times its acceleration. First, we sum the forces in the $x$ and $y$ directions and derive:

$$Pdy\left[\left(\frac{\partial \eta}{\partial x}\right)_{x+dx} - \left(\frac{\partial \eta}{\partial x}\right)_{x}\right] = P\frac{\partial^2 \eta}{\partial x^2}dxdy \tag{4.19}$$

and

$$Pdx\left[\left(\frac{\partial \eta}{\partial y}\right)_{y+dy} - \left(\frac{\partial \eta}{\partial y}\right)_{y}\right] = P\frac{\partial^2 \eta}{\partial y^2}dxdy\,. \tag{4.20}$$

Summing Equations 4.19 and 4.20 and setting them equal to the mass times the acceleration of the element, we get:

$$P\left[\frac{\partial^2\eta}{\partial x^2}+\frac{\partial^2\eta}{\partial y^2}\right]dxdy=\sigma\,dxdy\frac{\partial^2\eta}{\partial t^2} \tag{4.21}$$

Or, more compactly,

$$\frac{\partial^2\eta}{\partial x^2}+\frac{\partial^2\eta}{\partial y^2}=\frac{1}{c^2}\frac{\partial^2\eta}{\partial t^2}\ , \tag{4.22}$$

where, as in the derivation of the transverse dynamics in polar coordinates, we have $c=\sqrt{\frac{P}{\sigma}}$. The constant, $c$, is referred to as the wave speed of the membrane, and is dependent on only the tension and mass density. Notice that we can write Equation 4.22 as

$$\nabla^2\eta=\frac{1}{c^2}\frac{\partial^2\eta}{\partial t^2} \tag{4.23}$$

which looks identical to Equation 4.18; however, the Laplacian takes on a different form since we have changed coordinate systems. The fact that the Laplacian takes on different forms should not come as any surprise as we expect rectangular membranes to vibrate with parallel waves and circular membranes to vibrate with circular waves (like dropping a stone in a still bucket and watching the ensuing ripples emanate from the disturbance).

### 4.4 Motivating Physics for a More Complex Dynamics Model

Now that we have investigated the history of thin plate and membrane theory development, outlined the basic assumptions of both theories, and examined the equations of motion for transverse vibration for both theories, we must now decide what type of structural element we need to pursue with regards to space optics or radar apertures made from membrane-type materials under tensile loads. First, consider the

side profiles of two strips of material, one made from Kapton and the other from Upilex, hanging over the edge of a desk (as shown in Figure 4.9).

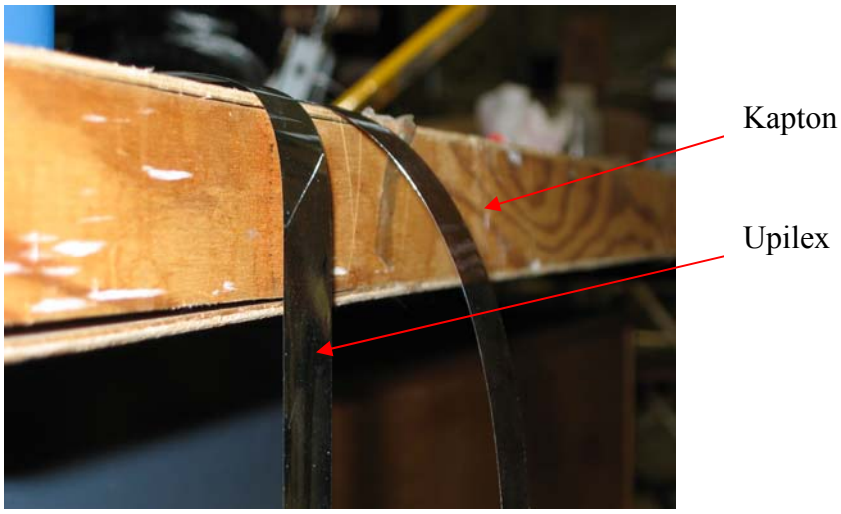


**Figure 4.9**. Strip samples of Kapton and Upilex hanging over the edge of a desk.

As shown in Figure 4.9, Kapton and Upilex demonstrate different mechanical properties. The Kapton strip shows more flexural rigidity as compared to the Upilex sample, and consequently would be classified as a thin plate (or, since it is a thin sample, a beam, since the 1-D equivalent of a thin plate is a beam element). The Upilex sample shows a small but negligible amount of flexural rigidity, and hence would be classified as a membrane (or a string, under the same argument as the Kapton sample). However, if we add active material to the two samples for the purpose of distributed actuation and vibration suppression, both membrane samples will have local mass and stiffness effects from the actuators and consequently behave like beams (in 1-D) or thin plates (in 2-D). From a modeling perspective, we would like to be able to capture the dynamics of the integrated systems in a similar fashion.

Williams, Inman, and Austin (2001) examined the possibility of modeling the interaction between a piezopolymer (PVDF) and the skin of an inflatable Kapton torus using membrane theory. In brief, the authors found that modeling layers of PVDF film attached to the surface of a planar Kapton structure using membrane theory could not

capture the added local stiffness of a PVDF patch. Consequently, the authors could not model the PVDF patch as an effective sensor. However, the PVDF patch was shown to be an effective sensor in experimental studies performed by Park, Ruggiero, and Inman (2002). Park, Ruggiero, and Inman (2002) used PVDF patches as sensors to perform an experimental modal analysis study on an inflated torus and identified both the damped natural frequencies and mode shapes of the structure. Hence, this is an example of how using pure membrane theory fails to capture the physics of the real system, and therefore evokes a need for a more advanced modeling technique.

In an attempt to address the modeling issue, let's look at the equation of motion governing the dynamics of a 1-D beam structure. A beam element is able to capture both the added mass and the added stiffness of an active piezoelectric element, unlike a membrane or string element. The equation of motion for the transverse deflection of a beam undergoing free vibration is given by:

$$\rho(x)A(x)\frac{\partial^2 w(x,t)}{\partial t^2}+\frac{\partial^2}{\partial x^2}\left[E(x)I(x)\frac{\partial^2 w(x,t)}{\partial x^2}\right]=0\ , \tag{4.24}$$

where *E(x)* is the elastic modulus, *I(x)* is the area moment of inertia, *ρ(x)* is the density, and *A(x)* is the cross-sectional area of the beam. Recall the equation of motion for a rectangular membrane element undergoing transverse free vibration, given by

$$P\left[\frac{\partial^2 \eta(x,y,t)}{\partial x^2}+\frac{\partial^2 \eta(x,y,t)}{\partial y^2}\right]=\rho(x)A(x)\frac{\partial^2 \eta(x,y,t)}{\partial t^2}\,. \tag{4.25}$$

For modeling purposes, it is proposed to augment the beam dynamics, Equation 4.24, with a 1-D equivalent of the membrane dynamics, Equation 4.25. Doing so yields

$$\rho(x)A(x)\frac{\partial^2 w(x,t)}{\partial t^2}-P\frac{\partial^2 w(x,t)}{\partial x^2}+\frac{\partial^2}{\partial x^2}\left[E(x)I(x)\frac{\partial^2 w(x,t)}{\partial x^2}\right]=0 \tag{4.26}$$

Equation 4.26 now contains a second order spatial term to account for the traveling wave properties experienced by membranes, and also contains the dynamics of a beam that includes a model for the flexural stiffness of the beam (through the inertial term *I(x)*). Further, for a thin membrane, the term *E(x)I(x)* is orders of magnitude smaller than the other parameters in Equation 4.26. Although the term *E(x)I(x)* is small, it is not assumed to be negligible, and also allows the dynamics of a piezoelectric sensor or actuator to be included (unlike the Williams, Inman, and Austin (2001) membrane model). For now, if we assume that the beam-membrane element is uniform throughout, then we arrive at the dynamic equation:

$$\frac{\partial^4 w(x,t)}{\partial x^4} - \frac{c^2}{EI}\frac{\partial^2 w(x,t)}{\partial x^2} + \frac{\rho A}{EI}\frac{\partial^2 w(x,t)}{\partial t^2} = 0 \qquad (4.27)$$

Of particular interest in Equation 4.27 is the magnitude of the membrane (or wave) term, $c^2 / EI$. As the magnitude of this term is increased beyond unity, the equation of motion is dominated by the wave equation and looks like a string. Conversely, as the magnitude approaches zero, the dynamics approach that of a beam. When the two terms are comparable, the element undergoes vibration that behaves like a beam but with the added complexity of a traveling wave.

Equation 4.27 is a form of the dynamics describing the transverse vibration of a beam under a uniform load. The solution to such a system is given by Shaker (1975). We will now derive the solution to Equation 4.27 and examine the effect the additional "membrane term" has on the dynamics of the structure.

### 4.5 Solution of the Beam under Uniform Tension Equation

First, to help simplify the solution process, let's rewrite Equation 4.27 as:

$$\frac{\partial^4 \overline{w}(x,t)}{\partial \overline{x}^4} - \overline{k}^2 \frac{\partial^2 \overline{w}(x,t)}{\partial \overline{x}^2} + \overline{\gamma}^2 \frac{\partial^2 \overline{w}(x,t)}{\partial t^2} = 0, \tag{4.28}$$

where $\overline{w} = \frac{w}{L}$, $\overline{x} = \frac{x}{L}$, $\overline{k}^2 = \frac{P}{EI}L$ , and $\overline{\gamma}^2 = \frac{\rho A}{EI}L$.

Note that a positive value of *P* refers to a tensile load in this equation, whereas a negative value refers to a compressive load. Next, we will use the method of separation of variables to solve Equation 4.28. In using the method of separation of variables, we assume that the solution to Equation 4.28 can be separated into two parts—spatial and temporal portions (Boyce and DiPrima, 2001). Thus, we assume that the solution looks like:

$$W(\overline{x},t) = X(\overline{x})T(t). \tag{4.29}$$

Plugging Equation 4.29 into Equation 4.28 yields

$$X(\overline{x})''''T(t) - \overline{k}^2 X(\overline{x})''T(t) + \overline{\gamma}^2 X(\overline{x})\ddot{T}(t) = 0, \tag{4.30}$$

where the primes on $X(\overline{x})$ indicate total differentiation with respect to $\overline{x}$ and the overdots on *T(t)* indicate total differentiation with respect to time, *t*. After some simple rearranging we get the equation

$$\frac{X(\overline{x})''''}{X(\overline{x})} - \overline{k}^2 \frac{X(\overline{x})''}{X(\overline{x})} + \overline{\gamma}^2 \frac{\ddot{T}(t)}{T(t)} = 0 \tag{4.31}$$

Now, we explicitly separate the spatial and temporal portions of Equation 4.31 and get

$$\frac{X(\bar{x})''''}{X(\bar{x})} - \bar{k}^2 \frac{X(\bar{x})''}{X(\bar{x})} = -\bar{\gamma}^2 \frac{\ddot{T}(t)}{T(t)} \tag{4.32}$$

Since the left and right sides of Equation 4.32 are functions of different variables, it is argued that each side must be a constant. Therefore, we get:

$$\frac{X(\bar{x})''''}{X(\bar{x})} - \bar{k}^2 \frac{X(\bar{x})''}{X(\bar{x})} = -\bar{\gamma}^2 \frac{\ddot{T}(t)}{T(t)} = \bar{\omega}^2 . \tag{4.33}$$

Next, we let

$$\bar{\beta}^4 = \frac{\bar{\omega}^2}{\bar{\gamma}^2}, \tag{4.34}$$

and upon plugging Equation 4.34 into Equation 4.33, we arrive at the temporal ordinary differential equation,

$$\ddot{T}(t) + \bar{\beta}^4 T(t) = 0, \tag{4.35}$$

the solution of which is given by:

$$T(t) = A\sin(\beta^2 t) + B\cos(\beta^2 t), \tag{4.36}$$

where $A$ and $B$ are constants of integration. Now, we can solve for the spatial portion of the solution given by the differential equation:

$$\bar{X}(\bar{x})'''' - \bar{k}^2 \bar{X}(\bar{x})'' + \bar{\beta}^4 \bar{X}(\bar{x}) = 0, \tag{4.37}$$

where, as defined previously, $\bar{X} = \frac{w}{L}$, $\bar{x} = \frac{x}{L}$, $\bar{k} = kL$, *and* $\bar{\beta} = \beta L$.

The solution to Equation 4.37 is given by:

$$\overline{X}(\overline{x}) = a_1 \sin(\alpha_2 \overline{x}) + a_2 \sinh(\alpha_1 \overline{x}) + a_3 \cos(\alpha_2 \overline{x}) + a_4 \cosh(\alpha_1 \overline{x}), \tag{4.38}$$

where $a_1$, $a_2$, $a_3$, and $a_4$ are also constants of integration to be determined from the initial conditions imposed on the differential equation, and $\alpha_1$ and $\alpha_2$ are constants given by:

$$\begin{aligned} \alpha_1 &= \sqrt{-\frac{\overline{k}^2}{2} + \sqrt{\frac{\overline{k}^4}{4} + \overline{\beta}^4}} \\ \alpha_2 &= \sqrt{\frac{\overline{k}^2}{2} + \sqrt{\frac{\overline{k}^4}{4} + \overline{\beta}^4}} \end{aligned} . \tag{4.39}$$

Next, we would like to solve for the natural frequencies and mode shapes of the system as given by the spatial solution, Equation 4.38. For the current analysis we will assume that both ends of the physical structure are pinned, which leads to the following boundary conditions:

$$\begin{aligned} &\overline{X}(0) = \overline{X}(1) = 0 \\ &\overline{X}(0)'' = \overline{X}(1)'' = 0 \end{aligned} . \tag{4.40}$$

Physically, Equations 4.40 represent that at a pinned end the non-dimensionalized structure does not displace and cannot support a moment. Plugging Equations 4.40 into Equation 4.38, we obtain a system of 4 linear, simultaneous equations with 4 unknowns, meaning there is a unique solution to the system. From linear algebra, we can derive the characteristic equation governing the natural frequencies and mode shapes of the pinned-pinned system by taking the determinant of the system of equations. Doing so yields the characteristic equation:

$$\left(\alpha_1^2 + \alpha_2^2\right)\sin(\alpha_2)\sinh(\alpha_1) = 0 . \tag{4.41}$$

The natural frequencies of the system are those values of $\omega^2$ (which are buried in $\alpha_1$ and $\alpha_2$) that satisfy Equation 4.41. Note, however, that of the three terms comprising the left side of Equation 4.41, only the term $\sin(\alpha_2)$ can satisfy the equation. Otherwise, the solution would require that $\alpha_1$ and $\alpha_2$ both be zero, which means that the system doesn't vibrate. Therefore, we have

$$\sin(\alpha_2) = 0\,, \tag{4.42}$$

giving us the equation

$$\alpha_2 = n\pi = \sqrt{\frac{\bar{k}^2}{2} + \sqrt{\frac{\bar{k}^4}{4} + \bar{\beta}^4}} \quad for\ n = 1,2,3... \tag{4.43}$$

Solving Equation 4.43 for $\bar{\beta}^4$ yields

$$\bar{\beta}^4 = \left(n^2\pi^2 + \frac{\bar{k}^2}{2}\right)^2 + \frac{\bar{k}^4}{4}\,, \tag{4.44}$$

and, upon further simplification, we get

$$\bar{\beta}^2 = \sqrt{\left(\bar{k}^2 n^2\pi^2 + n^4\pi^4\right)}\,. \tag{4.45}$$

For future reference, if we restore the units to Equation 4.45, then we get the equation:

$$\omega_n = +\frac{1}{L^2}\sqrt{\frac{EI}{\rho A}\left(\left(k^2L^2n^2\pi^2 + n^4\pi^4\right)\right)}\,. \tag{4.46}$$

Equation 4.45 now gives us an analytical means to understand the behavior of the natural frequencies of the system as the magnitude of the wave (or tensile) term $\bar{k}^2$ is increased. Since we are most interested in tensile loads, we will increase the magnitude of the $\bar{k}^2$ term. Figure 4.10 visually depicts the behavior of the natural frequencies as the magnitude of the wave term, or tensile load, is increased.

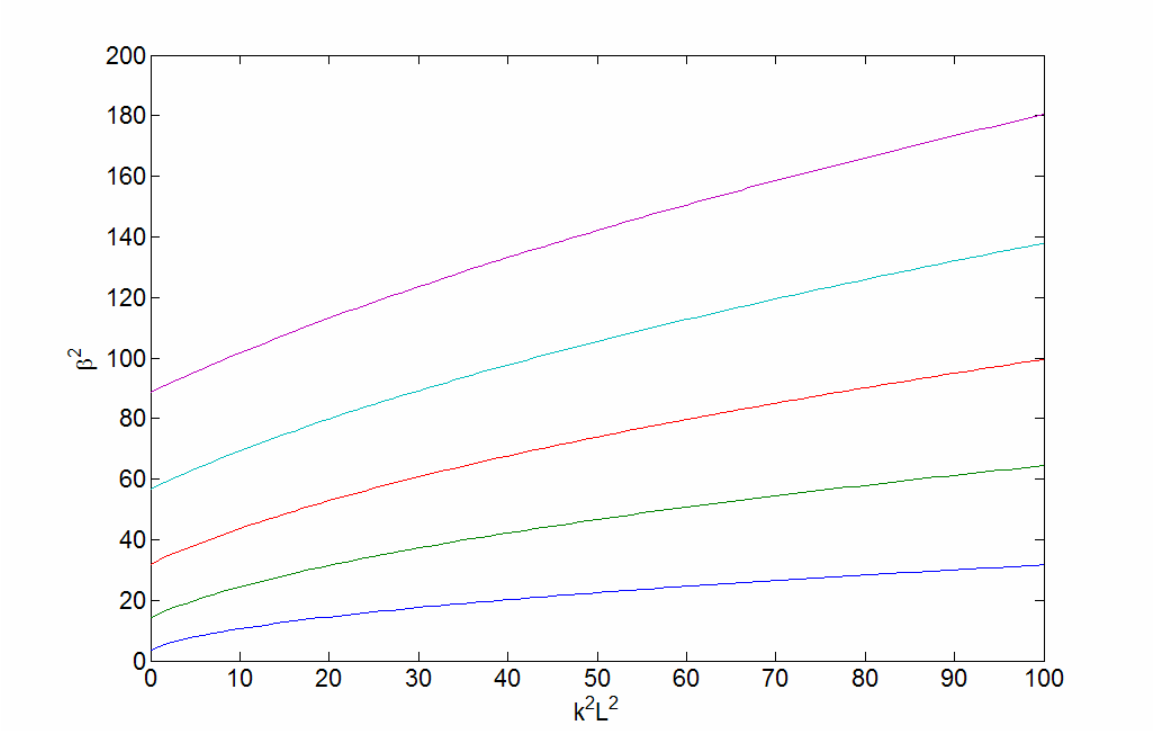


**Figure 4.10.** As the magnitude of the wave term $\bar{k}^2 = k^2 L^2$ is increased, the corresponding roots of the characteristic equation also increase.

The next chapter will show experimental validation of the above analysis, and verify the use of beam under uniform tension equation, Equation 4.27.

### 4.6 Chapter Summary

This chapter presents a historical summary of the work performed in the area of thin plate and membrane dynamic equation development. Although it is not a new contribution to the scientific community, it serves its purpose as a detailed summary distinguishing the nomenclature and nuances separating thin plates and membranes. All too often,

structural elements that are thin plates are incorrectly referred to as membranes and vice versa.

The materials under consideration for membrane mirrors are, in fact, membranes. They are subject to the limitations of membrane dynamics, and proper modeling of membrane optics must take into account such limitations. However, augmenting Kapton or Upilex with active material, like PZT, motivates us to consider a small but non-negligible amount of bending rigidity in our model. Consequently, we have augmented the transverse vibration equation of a beam with a wave (or string) term to capture both types of dynamics. This augmentation is important, as it now allows us to incorporate the more complex interaction between a piezoelectric bimorph or unimorph and a membrane sample. Such interaction cannot be modeled with pure membrane theory.

In summary, membranes differ from thin plates in that they: 1) cannot resist a bending load, due to their lack of flexural rigidity, and 2) can only sustain tensile loads, which consequently can lead to wrinkles. Keeping these differences in mind, we can now explore other aspects of membrane mirror design criteria in subsequent chapters. The next chapter will show experimental validation of the use of beam under uniform tension equation.